

A force-dependent switch reverses type IV pilus retraction

Berenike Maier^{*†}, Michael Koomey[‡], and Michael P. Sheetz^{*}

^{*}Department of Biological Sciences, Columbia University, 1212 Amsterdam Avenue, New York, NY 10027; and [‡]Center for Molecular Biology and Neuroscience and Department of Molecular Biosciences, Rikshospitalet, University of Oslo, N-0027 Oslo, Norway

Edited by A. Dale Kaiser, Stanford University School of Medicine, Stanford, CA, and approved June 14, 2004 (received for review April 1, 2004)

Type IV pilus dynamics is important for virulence, motility, and DNA transfer in a wide variety of prokaryotes. The type IV pilus system constitutes a very robust and powerful molecular machine that transports pilus polymers as well as DNA through the bacterial cell envelope. In *Neisseria gonorrhoeae*, pilus retraction is a highly irreversible process that depends on PilT, an AAA ATPase family member. However, when levels of PilT are reduced, the application of high external forces ($F = 110 \pm 10$ pN) induces processive pilus elongation. At forces of >50 pN, single pili elongate at a rate of $v = 350 \pm 50$ nm/s. For forces of <50 pN, elongation velocity depends strongly on force and relaxation causes immediate retraction. Both pilus retraction and force-induced elongation can be modeled by chemical kinetics with same step length for the rate-limiting translocation step. The model implies that a force-dependent molecular switch can induce pilus elongation by reversing the retraction mechanism.

Type IV pili are important virulence factors because they mediate bacterial adhesion to host mammalian cells (1) and horizontal gene transfer (2). These dynamic polymers elongate (3) and retract (4), most likely by polymerization and depolymerization into the inner membrane (5–7). Pilus dynamics and force generation depend on the presence of the pilus retraction protein PilT or its homologs (4). PilT increases infectivity with enteropathogenic *Escherichia coli* (8) and causes rearrangement of cytoskeletal proteins in host mammalian cells with *Neisseria gonorrhoeae* (1, 9). Furthermore, pilus dynamics mediates cell motility on surfaces (10) by a cycle of extension, attachment at the tip, and retraction. Twitching motility is necessary for the formation of *Pseudomonas aeruginosa* biofilms (11) and bacterial dispersal during infection of epithelial cells by *Neisseria* (12). *Neisseria* regulate the concentration of PilT during infection of host cells (7). Therefore, it is of major importance to understand the dynamics of pilus retraction and elongation at various levels of PilT.

Pilus elongation and retraction are controlled by PilF (13) and PilT (14), respectively. The PilF and PilT proteins are homologous with AAA ATPases, which include chaperones and mechanoenzymes. Like other AAA ATPases, PilT has a hexameric structure (15) and hydrolyzes ATP *in vitro* (16, 17). PilF is required for pilus polymerization, and PilT supports pilus retraction, most likely by depolymerization of the pilus.

Single pili generate forces exceeding 100 pN, and the velocity and force of pilus retraction is independent of the concentration of PilT (18). In WT *N. gonorrhoeae*, pilus retraction *in vitro* is a highly processive and irreversible process, indicating that the molecular motor powering pilus retraction is strongly bound to the pilus. Most molecular-transport systems translocate macromolecules through cell membranes only in one direction. Even DNA membrane translocation supported by type IV pilus proteins proceeds unidirectionally (19, 20). The sequence of type IV pilus elongation followed by retraction is required for twitching motility, and to our knowledge, reversals have not been reported. Nevertheless, there are circumstances during the process of infection in which elongation of retracting pili could prevent breakage and increase infectivity.

Here, we report the characterization of a force-dependent elongation process that is observed only when the levels of PilT are reduced. Force-dependent elongation appears to mirror the force–velocity relationship of retraction, suggesting that they depend on similar processes. We suggest that *in vivo* PilT levels participate in controlling the interaction between bacteria and host cells by controlling the tension on pili.

Materials and Methods

Bacterial Strains and Media. We used strains *N. gonorrhoeae* MS11 (WT) and its isogenic strain MS11-600 (*derepressible pilT*) (18). MW4 (*derepressible pilT*) was derived from N401 (*recA*[−]) and is described by Wolfgang *et al.* (21); to ensure that PCR did not alter the sequence, the ORF of *pilT* was sequenced (14, 21). GU5 (*pilU*) (22) was derived from N401 (*recA*[−]). All strains were maintained on Gc medium base (GCB) agar with supplements (Difco) and 0–0.1 mM isopropyl β -D-thiogalactoside (IPTG). Retraction assays were carried out in phenol red-free DMEM (GIBCO), supplemented with 2 mM L-glutamine/4 mM sodium pyruvate/5 mM ascorbic acid/1 mg/ml BSA/15 mM Hepes/0–0.1 mM IPTG, pH 7.9, at 33°C.

Retraction and Elongation Assay. For retraction experiments, 3- μ m silica beads (Polysciences) were coated with poly(L-lysine) and adsorbed to glass coverslips by centrifugation. We added 1.5 or 2 μ m carboxylated latex beads (Polysciences) without further treatment to a suspension of gonococci, mounted them on a microscope slide, and sealed them.

The optical tweezers system consisted of a Nd:YAG laser (2W), an inverted microscope (Zeiss), and a movable-mirror system that allowed computer-controlled deflection of the laser beam. Acquisition of positional data were performed as described by Simmons *et al.* (23) at a 1-kHz time resolution by using a quadrant photodiode (Hamamatsu, Bridgewater, NJ) and LABVIEW software (National Instruments, Austin, TX). Before each acquisition, the detector signal was calibrated by recording the response of bead movement due to triangular movement of the optical trap by the mirrors. Displacement was linear in a range of 400 nm. To check for linearity and record bead movements of >400 nm, we used an image acquisition system that contained a Nuvicon video camera (Dage-MTI, Michigan City, IN), an S-VHS video recorder, and a SGI workstation running ISEE particle-tracking software (Inovision, Durham, NC). We calibrated the trap stiffness by the viscous drag method, and we verified the calibration with a spectrum analysis of the Brownian motion of the bead.

Determination of Retraction Rate. The accuracy of the short-term rate of retraction is limited by the spatial fluctuations. Brownian

This paper was submitted directly (Track II) to the PNAS office.

Abbreviation: IPTG, isopropyl β -D-thiogalactoside.

[†]To whom correspondence should be sent at the present address: Institut für Experimentalphysik, Ludwig-Maximilians-Universität, Geschwister-Scholl Platz 1, 80539 Munich, Germany. E-mail: berenike.maier@physik.lmu.de.

© 2004 by The National Academy of Sciences of the USA

motion as well as an instability of the mirrors controlling the position of the laser beam generate an SD of $\sigma \approx 7\text{--}10\text{ nm}$. The oscillations of the mirror occur at multiples of 60 Hz; removing the peaks in the spectrum of the motion of the bead yields an SD of $\sigma \approx 4\text{ nm}$ at a trap stiffness of $k_{\text{trap}} = 0.3\text{ pN/nm}$. The amplitude of fluctuations is decreased when the pilus binds and retracts. To average the oscillations, we fitted a polygon to the data obtained from the photodetector with an average step length of 30 ms. We estimate the error in the velocity to be 2% because of Brownian motion (for details of this estimation, see ref. 24). To check whether increasing the integration time significantly influences the value obtained for the retraction rate, we compared the velocity-vs.-force curves obtained from 20 retraction events averaged over 30 or 100 ms. The data overlapped within the statistical error bars for $F > 20\text{ pN}$ (at lower forces, the start of a retraction is smeared out when the step length becomes large, resulting in a decreased velocity).

We assume that the major error in the measurement of retraction rates and stall force arises from the finite size of the bacterium and, thus, from a velocity and force component in the vertical direction, perpendicular to the coverslip. With a total distance of $3\text{ }\mu\text{m}$ between the center of the bead and the bacterium and an uncertainty of $\delta h \approx 0.5\text{ }\mu\text{m}$ in the height of the point of attachment of the pilus, we estimate an error of 15% in the retraction velocity and the stall force in the horizontal direction.

To assess the effect of the elasticity of bacterium and pilus on the velocity-vs.-force behavior, we corrected the retraction velocity according to $v_{\text{retract,elong}} = (1 + k_{\text{trap}}/k_{\text{bact}})v_{\text{bead}}$ (25), where $k_{\text{bact}} = 1.3 \pm 0.2\text{ pM/nm}$ (18). The stiffness of the bacterium and the pilus k_{bact} were obtained by measuring the extension of the pilus as a function of the external force in a PilT mutant.

The error in the retraction velocity, Δv , was calculated as a sum of the statistical error $v_s = \sigma_s/\sqrt{N}$, geometrical error $\Delta v_g = 0.15v$, and elastic error $\Delta v_e = 0.05v$ (i.e., $\Delta v = \Delta v_s + \Delta v_g + \Delta v_e$), where σ_s is the SD and N is the number of measurements.

Results

This bead-based assay allowed us to measure the retraction rate of a single type IV pilus and to apply external force to the retracting pilus (Fig. 1a). *N. gonorrhoeae* bacteria were immobilized by attachment to poly(L-lysine)-coated beads on a glass surface. A small latex bead was then brought to a bacterium by using an optical trap. Eventually, a pilus bound to the bead and pulled the bead out of the center of the laser trap. We measured the position of the bead at a frequency of 33 Hz. For deflections of the bead of $<400\text{ nm}$ from the trap center, the force acting on the bead increased linearly with the deflection. This assay has been shown (18) to measure the rate of pilus retraction at the level of a single pilus. Although more than one pilus could have bound to the bead simultaneously, the velocity-vs.-force relationship was the same for bacteria with one to three pili as for bacteria with many pili. This configuration was suitable to study pilus retraction, but pili were too flexible to measure significant assembly forces. However, we observed force-dependent pilus extension as relaxation of beads back to the center of the laser trap after retraction and force generation.

External Force Reverses Pilus Retraction. We used mutants (MS11-600, MW4) with a derepressible *pilT* gene encoding the PilT pilus retraction protein (0.1 mM IPTG induction level). In typical retraction experiments, the deflection d of the bead from the center of the optical trap increased as the pilus retracted (Fig. 1b). With increasing deflection, the force acting on the pilus increased and the rate of pilus retraction decreased until the stall force was reached (Fig. 1c and d). Subsequently, we observed that the beads moved back toward the center of the optical trap, indicating that the pilus elongated. With 0.1 M IPTG, the fraction of the stalled beads that elongated (p) was $83 \pm 5\%$ of

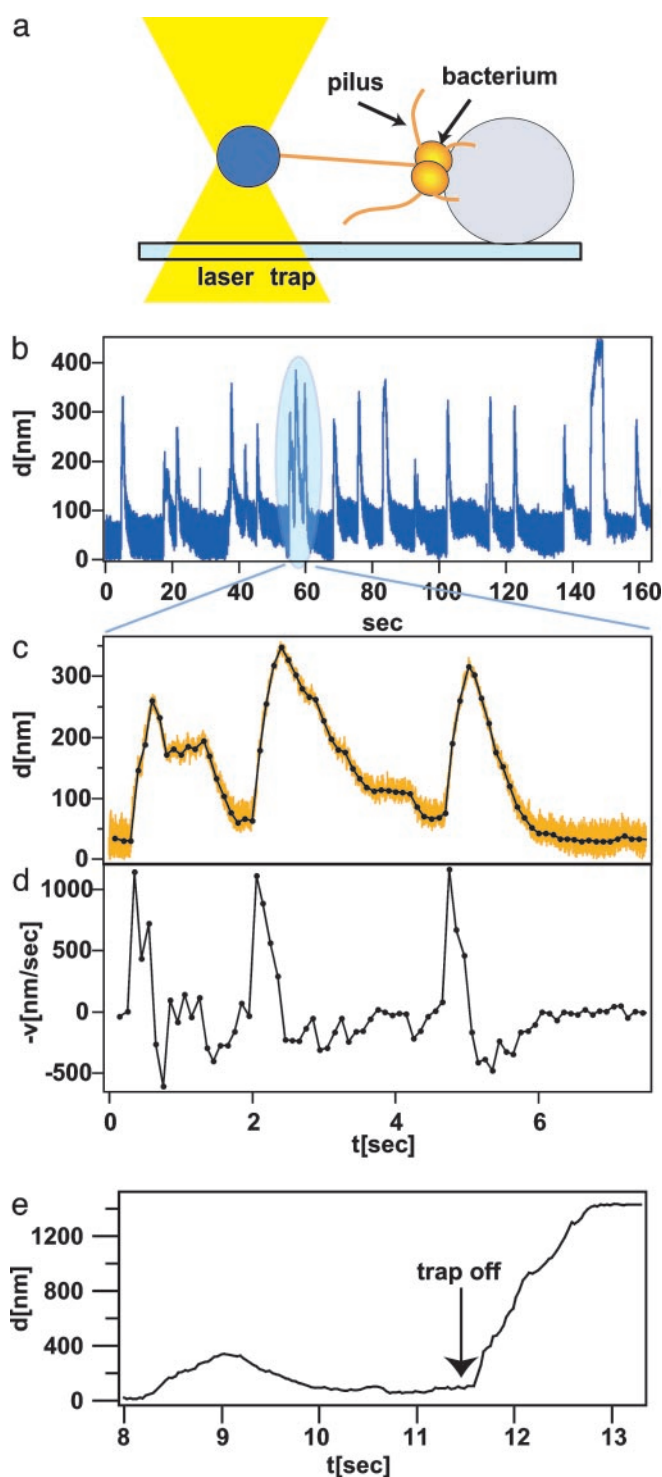


Fig. 1. Type IV pili elongate at high external force. (a) Setup. *N. gonorrhoeae* was immobilized on a glass coverslide by attachment to a poly(L-lysine) coated bead. A 1.5- or 2- μm latex bead was approached to the bacterium by using an optical trap. When a pilus bound the bead and retracted, the deflection of the bead from the center of the laser trap was measured by using a quadrant photodiode. (b) Example for pilus dynamics in the derepressible *pilT* mutant (MS11-600) at 0.1 mM IPTG. Pilus retraction deflects the bead from the center of the optical trap. When the maximum force is reached, the bead is moved back into the center of the optical trap. (c) Detail of the time series shown in a. The black line is a fit to the raw data (orange) with an average time period of 33 ms. (d) Velocity of bead deflection derived from the fit shown in c. (e) At 11.5 s the optical trap was turned off, and the pilus retracted immediately until the bead stuck to the bacterium ($n = 2$).

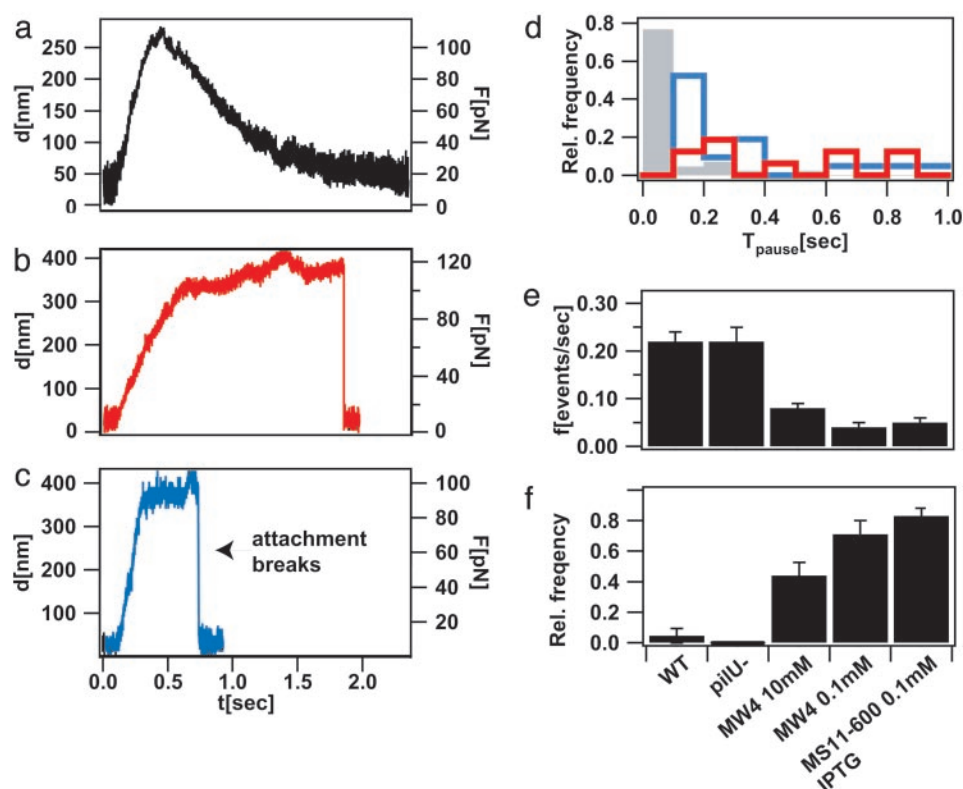


Fig. 2. Pilus elongation occurs only at reduced concentration of PilT. Typical pilus retraction events for derepressible *pilT* mutant at 0.1 mM IPTG (a), WT (b), and *pilU* mutant (c). (d) Distribution of pausing period before breaking event for WT and *pilU* mutant and distribution of pausing time before elongation event for derepressible *pilT* mutant. Gray bar, derepressible *pilT* at 0.1 mM IPTG ($n = 43$); red bar, WT ($n = 22$); blue bar, *pilU* ($n = 24$). (e) Frequency of retraction events. (f) Relative frequency of elongation events per total stalling events.

the total. Stalled beads were defined as those for which the velocity of pilus retraction dropped below $v = 40$ nm/s for at least 100 ms, and those beads experienced the maximum force. Note that during most retraction events the bacterium–pilus–bead complex broke at forces lower than the maximum force (for a histogram of breaking forces, see ref. 4). In contrast to the process of pilus retraction, pilus elongation showed a significant number of pauses on a time scale of $t > 50$ ms. In some cases, pili retracted again before the bead reached the center of the laser trap. When we turned the optical trap off during pilus elongation, the pili retracted immediately (Fig. 1e).

Force-Induced Pilus Elongation Requires Reduced Level of PilT. Pilus elongation was common in the derepressible *pilT* mutant (Fig. 2a) but not in the WT strain (Fig. 2b and f). In the 22 stalling events in WT bacteria, only one elongation was observed after a stalling duration of 2 s. In all other cases, the pilus tether between the bacterium and the bead broke without detectable pilus elongation. Fig. 2b shows that the position of the bead fluctuates around the maximum deflection; however, the pilus did not elongate a significant distance.

PilU is coexpressed from the same promoter as *pilT* (22), and it is reasonable to assume that the concentration of PilU is also decreased in the derepressible *pilT* strain. PilU is structurally related to PilT and other AAA ATPases, and it has been shown to play a role in epithelial cell adhesion and bacterial autoagglutination (22). To assess the role of PilU in pilus dynamics, we used a *pilU* knockout strain (GU5). In 24 stalling events, we did not observe a single pilus elongation event (Fig. 2c).

The question arises whether we did not observe pilus elongation in the WT or the *pilU* mutant because the attachment to the bead broke before the pilus elongated. Most stalling events

lasted for >0.2 s in the WT and the *pilU* mutant (Fig. 2d), and one attachment lasted for >60 s (data not shown). In most cases, elongation in the derepressible *pilT* mutant started without a significant delay; the average pause length was $\langle t_{\text{pause}} \rangle = 0.11 \pm 0.05$ s. In one case, the pilus stalled for 26 s before elongation. (This event was not included in the average value.)

With the derepressible *pilT* strain, the retraction frequency was low as compared with the WT or the *pilU* mutant (Fig. 2e), indicating that *pilT* concentration was strongly reduced at all IPTG induction levels. The ratio of retraction frequency at 10 mM IPTG, as compared with 0.1 mM IPTG, was $f_{10\text{mM}}/f_{0.1\text{mM}} = 2.0 \pm 0.3$ (Fig. 2e), and the elongation ratio was $p_{10\text{mM}}/p_{0.1\text{mM}} = 0.6 \pm 0.1$ (Fig. 2f). In the WT and the *pilU* mutant (i.e., at normal levels of PilT), we did not observe a significant number of elongation events. Thus, our observations suggest that the level of PilT controlled the frequency at which force-induced pilus elongation occurred.

Pilus retraction proceeded at a rate of $v(F < 50 \text{ pN}) = 1,200 \pm 200$ at forces of <50 pN. At forces of >50 pN, the retraction rate decreased exponentially to zero at the average stall force $F_{\text{max}} = 110 \pm 10$ pN. Neither the stall force (Fig. 3a) nor the velocity-vs.-force relationship of pilus retraction (Fig. 3b) were significantly altered from control values in the derepressible *pilT* mutant and the *pilU* mutant. This observation indicates that pilus retraction was normal in the mutant cells and that elongation was not reflecting a change in the retraction process. We cannot positively rule out that reduction of PilT level favors the formation or change in composition of heterohexamers of PilF and PilT. However, if reduction of PilT concentration were to favor the formation of heterohexamers, we would expect to find a change in the velocity-vs.-force relationship of pilus retraction that was not observed.

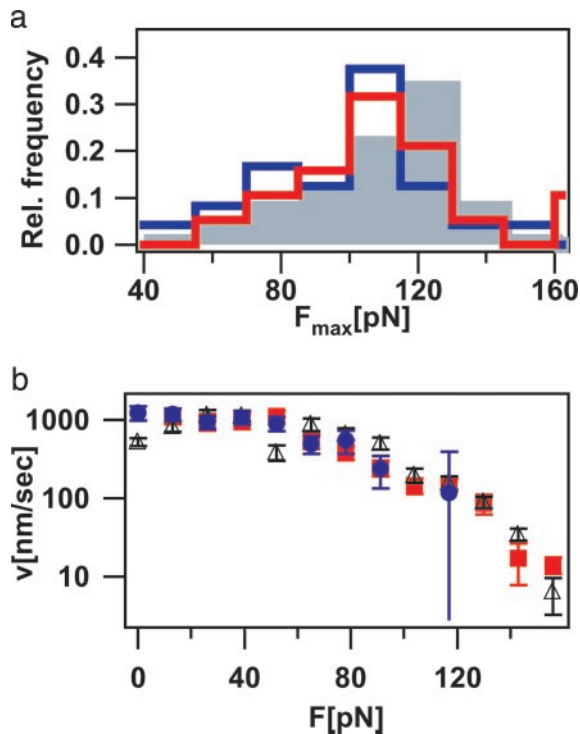


Fig. 3. Force-dependent kinetics of pilus retraction. (a) Distribution of maximum forces of derepressible *pilT* (MS11-600) at 0.1 mM IPTG ($n = 43$; gray bar), WT ($n = 22$; red bar), and *pilU* ($n = 24$; blue bar). (b) Velocity-vs.-force relationship for pilus retraction for derepressible *pilT* at 0.1 mM IPTG (triangle), WT (square), and *pilU* (circle).

Velocity-Vs.-Force Relationship in Pilus Elongation. Near the stall force, the average velocity of pilus elongation was $v = 350 \pm 50$ nm/s (Fig. 4a). As the force on the pilus dropped during elongation, the velocity of pilus elongation decreased only

minimally until the force reached 50 pN. When the force decreased below 50 pN, the decrease in velocity with force was fit with an exponential. This behavior is similar to pilus retraction, where the crossover force between constant velocity and exponential decay was at 50 pN (Fig. 4b). Thus, it appears that the process of extension is related to the process of retraction.

Discussion

The application of external force in combination with a reduced level of PilT induced force-dependent pilus elongation. We observed pilus elongation only in a derepressible *pilT* background and not in the WT or a *pilU* mutant. Force-dependent pilus elongation was initiated at the stall force, where the pilus retraction velocity in WT cells was nearly zero. After elongation began, the rate of pilus elongation was nearly constant with force until the force dropped to <50 pN. At <50 pN, the force-velocity relationship was nearly exponential. Thus, the processes of retraction and elongation mirror one another.

Molecular Model for Pilus Dynamics. To model pilus dynamics, it is important to understand the components that are involved. Fig. 4c shows the major proteins involved in pilus formation and retraction. For brevity, not all known proteins are discussed here. Pilin monomers have a hydrophilic head and a transmembrane, hydrophobic tail. They are stored in the inner membrane (7) where they are processed by prepilin peptidase PilD (13). PilF is required for processed pilin monomers (13) to assemble into a helix with 5-fold symmetry and a pitch of 4 nm per turn (26). In another bacterium, *Vibrio cholerae*, the pilus structure was shown to be a helix with 3-fold symmetry and a pitch of 4.5 nm (27). In both structures, the effective length of a pilin monomer in a pilus is on the order of 1 nm. The bacterium exports the pilus through PilQ, a pore in the outer membrane (28). PilT, is required for pilus retraction (14) and it is the drop in the level of PilT that correlates with an increase in the probability of extension at the stall force.

How does the reduced level of PilT expression result in a force-dependent extension process? First, force may induce

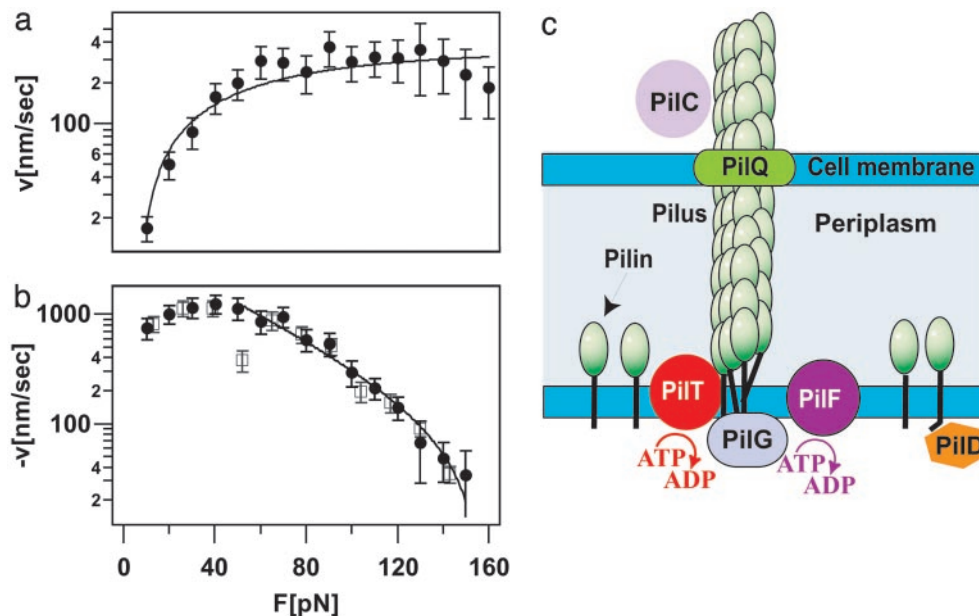


Fig. 4. A force-dependent switch. (a) Averaged velocity-vs.-force relationship for pilus elongation (MS11-600). The fit according to Eq. 1 yielded $a_e = 0.07 \pm 0.02$ nm and $A_e = 0.9 \pm 0.2$ ($\chi^2 = 13$, $\nu = 13$). (b) Averaged negative velocity-vs.-force relationship for pilus retraction in derepressible *pilT* mutant (MS11-600). To be able to fit the data, one data curve with a long stalling event at 50 pN was removed and data were averaged over a smaller force range (filled circles). The fit according to Eq. 1 yielded $a_r = 0.10 \pm 0.02$ nm/s and $A_r = 0.02 \pm 0.01$ ($\chi^2 = 5$, $\nu = 8$). (c) Molecular model of pilus formation.

dissociation of the pilus from PilT or other proteins in the membrane-attachment complex. We suggest that a single PilT complex is responsible for retracting a single pilus because the stall force does not depend on the concentration of the pilus retraction protein PilT and the frequency of retractions depends on the concentration of inducing agent (18). When the state of the complex is altered by force, it may be difficult to restore the retraction process unless a high concentration of PilT is present. In the WT, the concentration of PilT may be high enough to ensure rapid recruitment of PilT to the pilus, thus preventing pilus elongation. In the derepressible *pilT* strain, however, the concentration of PilT at the highest level of expression attainable is still 3–4 fold lower than that in WT strains. Thus, its level may be too low to ensure stabilization, and the pilus elongates. Direct interaction between PilT and the pilus has not been proven, and it has been suggested that PilT may have a regulatory role in pilus retraction (29). The same argument holds for any pilus-binding protein whose expression is regulated by the concentration of PilT. A second explanation for the effect of force on a molecular level would be that force altered the conformation of the molecular complex that drives pilus retraction (presumably PilT) and the presence of additional PilT molecules in the WT and *pilU* cells favors a cooperative transition to the retraction state.

Pilus elongation in the absence of external force requires PilF. By using fluorescence microscopy, Skerker and Berg (3) showed for *P. aeruginosa* that both pilus elongation and pilus retraction occur at $v_{e,r}(F=0) = 0.5 \mu\text{m/s}$ at 25°C in the absence of external force. The difference between the retraction rates measured in the fluorescence experiments and those measured here arises from the difference in temperature (B.M. and M.P.S., unpublished data). Fig. 4a shows $v_e(F=0) \ll 0.5 \mu\text{m/s}$, suggesting that pilus elongation in our experiments was purely force-induced. Because *pilF* mutants do not form pili, we were unable to assess the role of PilF directly in the observed elongation events. Because elongation stops and retraction resumes when the force drops to zero, we believe that the elongation process that we observe is distinct from elongation in the absence of external force.

The Elementary Step in Pilus Transport. Theoretical analyses can give a measure of the elementary step that leads to motion (30, 31), which is most likely the removal or addition of one pilin subunit from the pilus. In the absence of external force, pilus length changes at a velocity of $v = (k_+ - k_-)\delta$, where δ is the effective length of a pilin subunit in the pilus, k_+ is the rate of the rate-limiting step during polymerization, and k_- is the rate of the corresponding backward-step. We assume that the concentration of pilin subunits in the membrane is high enough that the concentration does not change significantly during the polymerization. This assumption should be valid, in particular when polymerization directly follows depolymerization, as was the case in our experiments. We set $k_+/k_- \equiv A$ without external force. In a quasiequilibrium approximation, we assume that application of external force leads to $k'_+/k'_- = A\exp(Fa/k_B T)$, where a is the average length of the rate-limiting mechanical step. The exponential factor may account for either a change in the height of an activation barrier of the rate-limiting step (i.e., a strain in the molecular motor that drives pilus transport) or a change in the relative levels of free energy between one pilin subunit in the membrane and one subunit in the pilus. Assuming that the available pilin concentration is large compared with the change in pilin concentration, the polymerization velocity is

$$v(F) = k'_+ \delta \left(1 - \frac{\exp(-Fa/k_B T)}{A} \right). \quad [1]$$

A best fit to the velocity-vs.-force relationship obtained for pilus elongation (Fig. 4a) yields $a_e = 0.07 \pm 0.03 \text{ nm}$ and $A_e \approx 1$. Fig.

4b shows the best fit to the velocity-vs.-force relationship for pilus retraction. The velocity is constant for forces of $<50 \text{ pN}$, suggesting that a nonmechanical step is rate limiting at low forces. We found that $a_r = 0.10 \pm 0.02 \text{ nm}$ at $F > 50 \text{ pN}$ and $A_r = 0.02 \pm 0.01$.

The values for the length of the rate-limiting step for pilus elongation and pilus retraction are within experimental error. A straightforward explanation for this observation would be that the molecule that switches between pilus elongation and pilus extension alters the free-energy difference between one pilin subunit added and one pilin removed. The change from $A_e \approx 1$ during elongation to $A_r \ll 1$ during retraction is in agreement with this hypothesis. This switch most likely alters the protein composition of the assembly–disassembly complex at the base of the pilus. Because the transition from retraction to elongation occurred only at a reduced level of PilT, it is tempting to speculate that unbinding of PilT or a protein that is regulated by PilT is responsible for the transition. Recent findings on bundle-forming pili in enteropathogenic *E. coli* (32) further support this suggestion. These studies showed that BfpD (PilF homolog), BfpC, and BfpE (PilG homolog) formed a complex that associated subsequently with BfpF (PilT homolog) in agreement with transient binding of BfpF to a complex at the base of the pilus.

In the theoretical analysis, the force acts on a length of $a \approx 0.1 \text{ nm}$, whereas one pilin subunit in the pilus has a length of $\delta \approx 1 \text{ nm}$. One explanation would be that pilus translocation occurs in two steps. The shorter step of 0.1 nm would then become rate-limiting at forces accessible in our experiment. Because our data are consistent with a single-exponential behavior, we suggest that the main translocation step would become rate-limiting at much larger forces than 100 pN . Another explanation can come from the fact that PilT forms a hexamer that hydrolyzes ATP (15). During one unit step, six ATPases may work in parallel.

Conclusion

The finding that force can cause extension of pili at low levels of PilT places important constraints on possible mechanisms of pilus retraction. In terms of possible explanations, we favor the hypothesis that force induces the separation of PilT from the normal retraction complex, which would allow elongation in the absence of high concentrations of PilT. Variation of PilT concentration, symmetry in the force-dependent extension and the retraction processes, and recent findings in enteropathogenic *E. coli* (32) reinforce the hypothesis that both external force and PilT dictate the direction of pilus dynamics.

What is the biological relevance of force-dependent pilus elongation? Force-induced pilus elongation releases the tension generated during pilus retraction. During infection, tissue movements of eukaryotic host cells may develop high tensions on the pilus. The bacterium–pilus–bead (and presumably also bacterium–pilus–host cell) complex is very fragile compared with the high forces generated during pilus retraction (4). Thus, force-induced pilus extension may be used to adjust the tension without breaking the pilus. Furthermore, pilus-induced tension has been proposed to be important for the cytoskeletal response of the host cell to adhesion of *Neisseria* (4). Vice versa, the level of PilT (7), and thus pilus dynamics, is regulated during infection. Therefore, it is tempting to speculate that PilT levels participate in controlling the interaction between bacteria and host cells by controlling the tension.

We thank Laura Potter, Maggie So, and Alexey Merz for helpful discussions. B.M. was supported by the Deutsche Forschungsgemeinschaft (Emmy Noether Program), and M.K. was supported by funds from the Norwegian Research Council. This work was supported by National Institutes of Health Grant GM23354.

1. Merz, A. J. & So, M. (2000) *Annu. Rev. Cell Dev. Biol.* **16**, 423–457.
2. Aas, F. E., Wolfgang, M., Frye, S., Dunham, S., Lovold, C. & Koomey, M. (2002) *Mol. Microbiol.* **46**, 749–760.
3. Skerker, J. M. & Berg, H. C. (2001) *Proc. Natl. Acad. Sci. USA* **98**, 6901–6904.
4. Merz, A. J., So, M. & Sheetz, M. P. (2000) *Nature* **407**, 98–102.
5. Kaiser, D. (2000) *Curr. Biol.* **10**, R777–R780.
6. Merz, A. J. & Forest, K. T. (2002) *Curr. Biol.* **12**, R297–R303.
7. Morand, P. C., Bille, E., Morelle, S., Eugene, E., Beretti, J. L., Wolfgang, M., Meyer, T. F., Koomey, M. & Nassif, X. (2004) *EMBO J.* **23**, 2009–2017.
8. Bieber, D., Ramer, S. W., Wu, C. Y., Murray, W. J., Tobe, T., Fernandez, R. & Schoolnik, G. K. (1998) *Science* **280**, 2114–2118.
9. Lee, S. W., Bonnah, R. A., Higashi, D. L., Atkinson, J. P., Milgram, S. L. & So, M. (2002) *J. Cell Biol.* **156**, 951–957.
10. Sun, H., Zusman, D. R. & Shi, W. (2000) *Curr. Biol.* **10**, 1143–1146.
11. Singh, P. K., Parsek, M. R., Greenberg, E. P. & Welsh, M. J. (2002) *Nature* **417**, 552–555.
12. Pujol, C., Eugene, E., Marceau, M. & Nassif, X. (1999) *Proc. Natl. Acad. Sci. USA* **96**, 4017–4022.
13. Freitag, N. E., Seifert, H. S. & Koomey, M. (1995) *Mol. Microbiol.* **16**, 575–586.
14. Wolfgang, M., Lauer, P., Park, H. S., Brossay, L., Hebert, J. & Koomey, M. (1998) *Mol. Microbiol.* **29**, 321–330.
15. Forest, K. T., Satyshur, K. A., Worzalla, G. A., Hansen, J. K. & Herdendorf, T. J. (2004) *Acta Crystallogr. D* **60**, 978–982.
16. Herdendorf, T. J., McCaslin, D. R. & Forest, K. T. (2002) *J. Bacteriol.* **184**, 6465–6471.
17. Okamoto, S. & Ohmori, M. (2002) *Plant Cell Physiol.* **43**, 1127–1136.
18. Maier, B., Potter, L., So, M., Long, C. D., Seifert, H. S. & Sheetz, M. P. (2002) *Proc. Natl. Acad. Sci. USA* **99**, 16012–16017.
19. Dubnau, D. (1999) *Annu. Rev. Microbiol.* **53**, 217–244.
20. Maier, B., Chen, I., Dubnau, D. & Sheetz, M. P. (June 6, 2004) *Nat. Struct. Mol. Biol.*, 10.1038/nsmb783.
21. Wolfgang, M., Park, H. S., Hayes, S. F., van Putten, J. P. & Koomey, M. (1998) *Proc. Natl. Acad. Sci. USA* **95**, 14973–14978.
22. Park, H. S., Wolfgang, M. & Koomey, M. (2002) *Infect. Immun.* **70**, 3891–3903.
23. Simmons, R. M., Finer, J. T., Chu, S. & Spudich, J. A. (1996) *Biophys. J.* **70**, 1813–1822.
24. Maier, B., Bensimon, D. & Croquette, V. (2000) *Proc. Natl. Acad. Sci. USA* **97**, 12002–12007.
25. Gittes, F. & Schmidt, C. F. (1998) *Methods Cell Biol.* **55**, 129–156.
26. Parge, H. E., Forest, K. T., Hickey, M. J., Christensen, D. A., Getzoff, E. D. & Tainer, J. A. (1995) *Nature* **378**, 32–38.
27. Craig, L., Taylor, R. K., Pique, M. E., Adair, B. D., Arvai, A. S., Singh, M., Lloyd, S. J., Shin, D. S., Getzoff, E. D., Yeager, M., *et al.* (2003) *Mol. Cell* **11**, 1139–1150.
28. Collins, R. F., Ford, R. C., Kitmitto, A., Olsen, R. O., Tonjum, T. & Derrick, J. P. (2003) *J. Bacteriol.* **185**, 2611–2617.
29. Wolfgang, M., van Putten, J. P., Hayes, S. F., Dorward, D. & Koomey, M. (2000) *EMBO J.* **19**, 6408–6418.
30. Fisher, M. E. & Kolomeisky, A. B. (1999) *Proc. Natl. Acad. Sci. USA* **96**, 6597–6602.
31. Peskin, C. S., Odell, G. M. & Oster, G. F. (1993) *Biophys. J.* **65**, 316–324.
32. Crowther, L. J., Anantha, R. P. & Donnenberg, M. S. (2004) *Mol. Microbiol.* **52**, 67–79.